Published OnlineFirst June 18, 2019; DOI: 10.1158/1535-7163.MCT-18-1250

Small Molecule Therapeutics

Molecular Cancer Therapeutics

Encapsulation of Temozolomide in a Calixarene Nanocapsule Improves Its Stability and Enhances Its Therapeutic Efficacy against Glioblastoma

Alexander Renziehausen[1], Antonis D. Tsiailanis[2], Richard Perryman[1], Evgenios K. Stylos[2,3], Christos Chatzigiannis[2], Kevin O'Neill[1], Timothy Crook[4], Andreas G. Tzakos[2], and Nelofer Syed[1]

Abstract

The alkylating agent temozolomide (TMZ) is the first-line chemotherapeutic for glioblastoma (GBM), a common and aggressive primary brain tumor in adults. However, its poor stability and unfavorable pharmacokinetic profile limit its clinical efficacy. There is an unmet need to tailor the therapeutic window of TMZ, either through complex derivatization or by utilizing pharmaceutical excipients. To enhance stability and aqueous solubility, we encapsulated TMZ in a p-sulphonatocalix[4]arene (Calix) nanocapsule and used ^{1}H-NMR, LC-MS, and UV–Vis spectroscopy to chart the stability of this novel TMZ@Calix complex according to FDA and European Medicines Agency guidelines. LC-MS/MS plasma stability assays were conducted in mice to further explore the stability profile of TMZ@Calix *in vivo*. The therapeutic efficacy of TMZ@Calix was compared with that of unbound TMZ in GBM cell lines and patient-derived primary cells with known O6-methylguanine-DNA methyltransferase (*MGMT*) expression status and *in vivo* in an intracranial U87 xenograft mouse model. Encapsulation significantly enhanced the stability of TMZ in all conditions tested. TMZ@Calix was more potent than native TMZ at inhibiting the growth of established GBM cell lines and patient-derived primary lines expressing *MGMT* and highly resistant to TMZ. *In vivo*, native TMZ was rapidly degraded in mouse plasma, whereas the stability of TMZ@Calix was enhanced threefold with increased therapeutic efficacy in an orthotopic model. In the absence of new effective therapies, this novel formulation is of clinical importance, serving as an inexpensive and highly efficient treatment that could be made readily available to patients with GBM and warrants further preclinical and clinical evaluation.

Introduction

Temozolomide (TMZ) is used for the treatment of primary brain tumors and brain metastases. It is the first-line chemotherapeutic for glioblastoma (GBM), which is the most common and aggressive malignant primary brain tumor. Radiotherapy with concomitant TMZ following surgical resection of the tumor is considered standard therapy for GBM, and in this combination the contribution of TMZ is an increase in the median overall survival of 2.5 months (1, 2). TMZ is a prodrug for the metabolite 5-(3-methyltriazen-1-yl)imidazole-4-carboxamide (MTIC), which acts as an alkylating agent to deliver a methyl group to the N-7 or O-6 position of guanine residues in the DNA. This DNA damage leads to inhibition of DNA replication and ultimately cell-cycle arrest (3). However, the O6-methylguanine adduct can be repaired by O6-methylguanine-DNA methyltransferase (MGMT), which confers TMZ resistance to approximately 60% of GBM tumors that express it (4–6). Despite this high incidence of inherent or acquired resistance, TMZ remains the main chemotherapeutic used against GBM. This is largely due to its pharmacokinetic characteristics and biodistribution. It has 100% oral bioavailability, a rapid absorption with a t_{max} of approximately 1 hour, and due to its small size (194 Da) it is able to cross the blood–brain barrier (BBB; refs. 7–9).

Unfortunately, TMZ has some unfavorable characteristics that greatly limit its clinical potential. Although it is stable at acidic pH, under slightly alkaline conditions it is rapidly hydrolyzed to MTIC, and this active alkylating agent rapidly degrades to the methyl diazonium cation and the metabolite 5-aminoimidazole-4-carboxamide (AIC; Fig. 1). Compared with TMZ, MTIC has poor BBB penetration and reduced cellular uptake (10). Therefore, the accumulation of therapeutically effective amounts of MTIC at the site of the tumor relies on the stability of TMZ and its delivery past the BBB. However, due to the rapid elimination rate and short half-life of only around 1.8 hours, the majority of the administered TMZ never reaches the tumor. In fact, only around 20% of the administered dose of TMZ is generally

[1]John Fulcher Neuro-Oncology Laboratory, Imperial College London, Hammersmith Hospital, London, UK. [2]Section of Organic Chemistry and Biochemistry, Department of Chemistry, University of Ioannina, Ioannina, Greece. [3]Biotechnology Laboratory, Department of Biological Applications and Technology, University of Ioannina, Ioannina, Greece. [4]Department of Oncology, St. Luke's Cancer Institute, Royal Surrey County Hospital, Guildford, UK.

Note: Supplementary data for this article are available at Molecular Cancer Therapeutics Online (http://mct.aacrjournals.org/).

A. Renziehausen, A.D. Tsiailanis, A.G. Tzakos, and N. Syed contributed equally to this article.

Corresponding Author: Nelofer Syed, John Fulcher Neuro-Oncology Laboratory, Imperial College London, Burlington Danes, Hammersmith Campus, Du Cane Road, W12 0NN London, UK. Phone: 44-20-7594-5292; E-mail: n.syed@imperial.ac.uk

Mol Cancer Ther 2019;18:1497–505

doi: 10.1158/1535-7163.MCT-18-1250

Published OnlineFirst June 18, 2019; DOI: 10.1158/1535-7163.MCT-18-1250

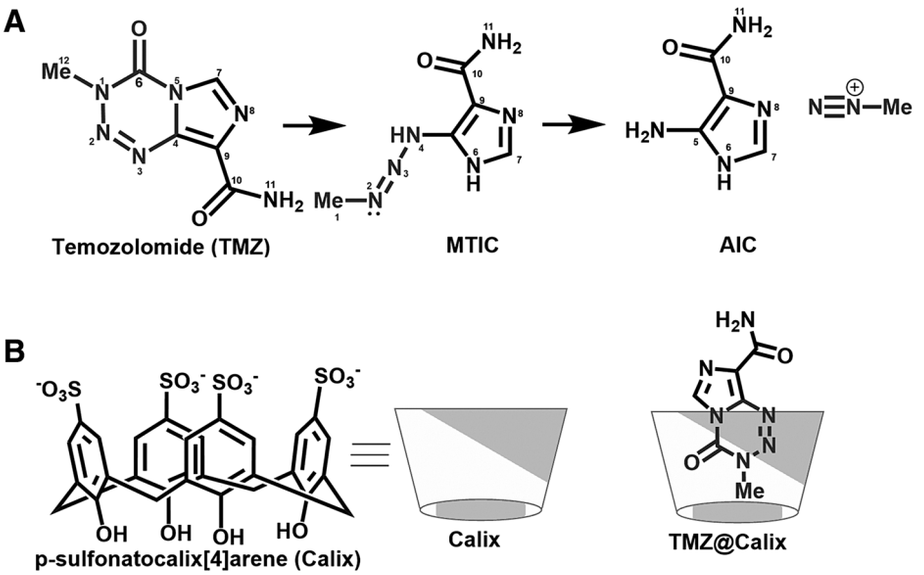

Figure 1.
Degradation products of native TMZ and structure of the TMZ@calixarene nanocapsule complex. **A,** Under neutral or alkaline conditions, TMZ undergoes rapid hydrolytic ring opening to produce the active metabolite MTIC ($t_{1/2} = 8$ min at pH = 7.4), the inactive metabolite AIC, and the active electrophile methyl diazonium cation ($t_{1/2} = 8$ s at pH = 7.4). **B,** Schematic representations of the calixarene (Calix) nanocapsule used in this study and the TMZ@Calix complex.

detectable in the cerebrospinal fluid at peak concentrations (11). High doses of TMZ need to be repeatedly administered to achieve the desirable antitumor effect, which leads to severe side effects, of which the most clinically significant is myelosuppression.

Stabilization of TMZ's core to achieve a longer plasma half-life could enable a dosing regimen with the same treatment benefits, but without negatively impacting the patient's quality of life. TMZ has previously been stabilized by loading it onto functionalized nanoparticles, nanoliposomes, or nanotubes, resulting in a more effective chemotherapeutic in various tested models (12–20). However, nanoparticles have numerous drawbacks that reduce their clinical potential, such as generally low drug-loading efficiencies, undefined toxicity profiles, and a high production cost (21). To achieve stabilization of TMZ while avoiding these drawbacks, we explored the water-soluble p-sulfonatocalix[4]arene (Calix) as a carrier due to its low toxicity, lack of immunogenicity, and its high aqueous solubility (22–25). Furthermore, Calix has a hydrophobic core that can accommodate the methyl group of the imidazotetrazine ring of TMZ and thereby protect it from rapid hydrolysis. This is important because this methyl group is key for the DNA-damaging activity of TMZ. Calix is known to improve the stability of guest molecules, as well as their solubility (26, 27). It has been used to enhance the stability, aqueous solubility, and efficacy of anticancer agents' paclitaxel, imatinib, and of dinuclear platinum complexes (28–30). Its applications in cancer chemotherapy have been reviewed previously (31). Here, we developed a formulate of TMZ and Calix with the aim of enhancing the stability of TMZ and improving its absorption profile to ultimately enhance its therapeutic efficacy.

Materials and Methods

Preparation of the TMZ@Calix inclusion complex

Ten milligrams (1 eq) of p-sulphonatocalix[4]arene (Sigma-Aldrich) was dissolved in 3 mL phosphate buffer pH 7.0 (10 μmol/L). 4 mg (1.5 eq) of TMZ (Sigma-Aldrich) was diluted in 300 μL MeOH. The solutions were mixed and magnetically stirred at room temperature for 1 hour. The contents were filtered through nylon filter with 0.45-μm pore size. Aqueous phase was evaporated under high vacuum giving the TMZ@Calix complex. Determination of encapsulated TMZ was performed using UV–Vis spectroscopy as described by Ishaq and colleagues (32). Generally, 1 mg TMZ@Calix complex contained 100 μg TMZ.

NMR spectroscopy

^{1}H-NMR spectra of calixarene, TMZ, and the complex were recorded in a Bruker 400 MHz Advance spectrometer using D_2O and DMSO-d_6 as solvents. Samples were dissolved in 500 μL D_2O and transferred to 5-mm NMR tubes warmed to 28°C. Topspin 3.1 was used to control the NMR system.

UV–Vis spectroscopy

The UV–Vis spectra of the TMZ@Calix complex were recorded with a PerkinElmer Lambda 25 spectrometer (slit = 1, speed 240 nm/min) at room temperature. The samples were dissolved in LC-MS grade H_2O and incubated under shaking at 37 ± 0.1°C at 600 rpm. Samples were centrifuged for 5 minutes, and precipitated TMZ was filtered off through regenerated cellulose syringe filters of a 0.20-μm pore size.

UHPLC-MS/MS buffer stability assay

Reversed phase liquid chromatography was performed using an Advance Ultra High Performance Liquid Chromatography (UHPLC) system (Bruker). For the ionization and detection of TMZ and IS, EVOQ Elite ER triple quadrupole mass spectrometer (Bruker) was operated in positive ionization electrospray mode (ESI) in multiple reaction monitoring. To evaluate the stability of TMZ in its encapsulated form, stability studies were conducted at pH 2.1, 4.5, and 7.1 at 37°C according to the FDA and European Medicines Agency (EMA) guidelines (33). Ten microliters of TMZ@Calix (30 μmol/L) was added to 280 μL hydrochloric acid (HCl, pH 2.1) and incubated at 37°C in a shaking bath. At time intervals of 0, 2, 4, 6, 8, 16, and 24 hours, the samples were removed from the bath and 10 μL of IS (27 μmol/L) was added, vortex-mixed, and transferred to LC-MS vials for analysis. The same procedure was followed for the samples incubated in ammonium formate (pH 4.5) and phosphate buffer (pH 7.1). To compare the stability of TMZ@Calix and TMZ, the same

Published OnlineFirst June 18, 2019; DOI: 10.1158/1535-7163.MCT-18-1250

experiments were also conducted for TMZ. All samples were studied in triplicate and the percentage of fraction remaining of TMZ against incubation time was plotted.

Cell culture

This study was approved by the Imperial College London Research and Ethics Committee (REC 14/EE/0024).

GBM cells were maintained at 37°C in a 5% CO_2 humidified incubator. Established GBM cell lines (8MG passage 8, U87 passage 8) were cultured in DMEM supplemented with 10% FBS. Cell lines were originally purchased from ATCC in 2014, expanded and stored as master stocks at low passage number (between 1 and 4). Master stocks were expanded into working stocks for use in experiments and did not exceed passage numbers beyond 20. Cells were maintained in cultures for less than 6 to 8 continuous weeks and tested for *Mycoplasma* contamination on a regular basis using the Mycoplasma Detection Kit quick test (Stratech Scientific UK). Patient-derived primary GBM cell cultures (GBM31, GBM59, and GBM77) were established from fresh tumor tissue obtained from first surgical debulking or stereotactic biopsies at Charing Cross Hospital. Tissue samples were provided by the Imperial College Healthcare NHS Trust Tissue Bank, which is supported by the National Institute for Health Research Biomedical Research Centre based at Imperial College Healthcare NHS Trust and Imperial College London. Tumors were washed in DMEM:F12 (1:1; Thermo Fisher Scientific, USA) and minced through a 100-μm cell strainer (Corning) to obtain a single-cell suspension. Cells are then centrifuged at 300 × *g* for 5 minutes and resuspended in sterile dH_2O to lyse contaminating red blood cells prior to being cultured in DMEM:F12 supplemented with 10% FBS (34).

qPCR analysis of *MGMT* expression

Total RNA was extracted using the RNeasy mini kit (Qiagen) and 2 μg converted to cDNA following the M-MLV Reverse Transcriptase protocol (Promega) according to the manufacturer's instructions. Samples were analyzed in triplicate with SYBR Select qPCR master mix (Thermo Fisher Scientific) using 50 ng of cDNA template for MGMT expression on a CFX96 Thermocycler (Bio-Rad) according to the manufacturer's instructions (*MGMT* forward primer: 5′-GGGTCTGCACGAAATAAAGC-3′; Reverse primer: 5′-TCCGGACCTCCGAGAAC-3′). Expression data were normalized to the mean Ct value of the reference gene hypoxanthine phosphoribosyltransferase 1 (*HPRT1*) and presented as $2^{-\Delta Ct}$.

In vitro cytotoxicity: sulforhodamine B and Cell Counting Kit 8 assays

Cells were seeded in 96-well plates (Corning) at 2×10^3 cells per well in their respective culture medium supplemented with 2% FBS. Twenty-four hours post-plating cells were treated with TMZ, Calix, physical mixture of TMZ and Calix or the TMZ@Calix complex in culture medium supplemented with 2% FBS. The concentration of TMZ in the complex was 100 μg TMZ/mg complex). To determine the IC_{50} of native TMZ, cells were treated with 2, 4, 8, 16, 32, 64, 128, 256, 512 μmol/L TMZ and analyzed for proliferation using sulforhodamine B (SRB) assay 9 days post-treatment as previously described (34). For experiments comparing the efficacy of the calixarene complex with native TMZ, doses just below the IC_{50} of native TMZ were used (5 μmol/L and 10 μmol/L for U87 and 8MG, respectively; 100 μmol/L and 200 μmol/L for the primary lines), and the equivalent equimolar concentrations of the complex were calculated and used. These experiments were harvested on days 6 and 9 post-treatment, and cell proliferation was analyzed by SRB for the established GBM cell lines and by the Cell Counting Kit 8 (CCK8, Sigma-Aldrich) for the primary lines according to the manufacturer's instructions.

In vivo pharmacokinetic analysis

Animal procedures were approved by the Animal Welfare and Ethical Review Body (Imperial College London). C57BL/6 female mice ages 6 weeks (Charles River Laboratories) were separated into two groups ($n = 3$) and injected intraperitoneally either with a single dose of TMZ (30 mg/kg) or a single dose of the TMZ@Calix complex (205.5 mg/kg, equivalent to 30 mg/kg of unbound TMZ). Blood was collected by cardiac puncture prior to treatment (day 0) and then at 0.5, 2, and 4 hours post-treatment in tubes containing heparin. Samples were centrifuged at 2862 × *g* for 10 minutes to separate the plasma which was acidified (pH < 4) with phosphoric acid 85%. All samples were stored at −80°C until further processing. To prepare samples for analysis 200 μL IS solution (theophylline 1 μg/mL in methanol) and 200 μL of 10 mmol/L pH 3.5 ammonium formate buffer were added to 100 μL of acidified mouse plasma, and this mixture was then precipitated with a 100 mmol/L 1:1 methanol:zinc sulfate solution. Following a vortex mix for 1 minute and centrifugation at 21,885 × *g* for 15 minutes, the supernatant was transferred to glass vials and TMZ was quantified by LC-MS/MS as described previously (35)

In vivo therapy of U87 intracranial xenografts

CD1 Swiss nude female mice 6 weeks old (Charles River Laboratories) were stereotactically injected with 3×10^5 U87-GFP/Luc cells into the right cerebral cortex ($n = 12$). Coordinates for injection were determined from the bregma (anteroposterior: +0.1; mediolateral: −0.2; dorsoventral: −0.3). Mice were first imaged 9 days after cell implantation and randomized into three treatment groups ($n = 4$): p-sulphonatocalix[4]arene only control (175.5 mg/kg), TMZ (30 mg/kg), and TMZ@Calix (205.5 mg/kg), which were carried out by intraperitoneal injections on days 13, 15, and 17 post-implantation. Prior to treatment, mice were weighed and the dose adjusted accordingly. Tumor development was followed by bioluminescent imaging on days 16, 20, 24, and 27. Animals were sacrificed on day 28 and perfused with ice-cold 4% PFA in PBS before brains were extracted and fixed in 4% PFA in PBS for 1 week. Brains were then transferred to 30% sucrose overnight and then frozen in 2-methylbutane (Sigma). Frozen brains were suspended in OCT compound (VWR), and whole brains were cut into 20-μm thick sections as depicted in Fig. 4C using a CM1900 Cryostat (Leica Biosystems) onto SuperFrost Plus microscope slides (VWR) and stained with hematoxylin and eosin (H&E). Images of H&E-stained sections were acquired using a Nikon Eclipse E800 microscope (Nikon) and the Surveyor imaging software (Objective Imaging).

Statistical analysis

One-way and two-way ANOVA were performed in GraphPad Prism software (version 7.0). Data are presented as mean ± standard error of the mean (SEM).

Published OnlineFirst June 18, 2019; DOI: 10.1158/1535-7163.MCT-18-1250

Results

Encapsulation of TMZ into Calix greatly enhances its stability

TMZ is the only FDA-approved drug for the treatment of GBM. However, due to its short half-life (2 hours), it has to be administered repeatedly and at high doses. To address these limitations, we encapsulated TMZ with Calix and tested its stability and solubility using ^{1}H-NMR spectroscopy, LC-MS/MS, and UV–Vis spectroscopy. We detected a significant chemical shift in the NMR spectrum of the TMZ@Calix complex compared with native TMZ indicating that the imidazotetrazine ring of TMZ was incorporated deep inside the hydrophobic cavity (Supplementary Fig. S1). We next analyzed the 1H-NMR spectrum for the presence of MITC (represented by the 7-H proton), which is highlighted in gray in Fig. 2A. There was an increase in signal at 7.23 ppm (1H, 7-H), indicating degradation of native TMZ to MTIC. Moreover, the methyl region of the spectrum indicated a decomposition of the singlet peak which is normally representative of intact TMZ (δ 4 ppm, 3H, 12-H). These changes were not detected in the TMZ@Calix ^{1}H-NMR spectrum, suggesting no detectable degradation of TMZ in this complex.

To further validate this enhanced stability under physiologic conditions, the degradation rate of TMZ and TMZ@Calix was monitored by LC-MS/MS and UV–Vis in aqueous buffer solutions of differing pH (Fig 2B and C). These pH values were selected to mimic the conditions present during gastrointestinal (GI) absorption after oral drug administration. Under fasting conditions, the pH range in the GI tract varies from 1.4 to 2.1 in the stomach, 4.9

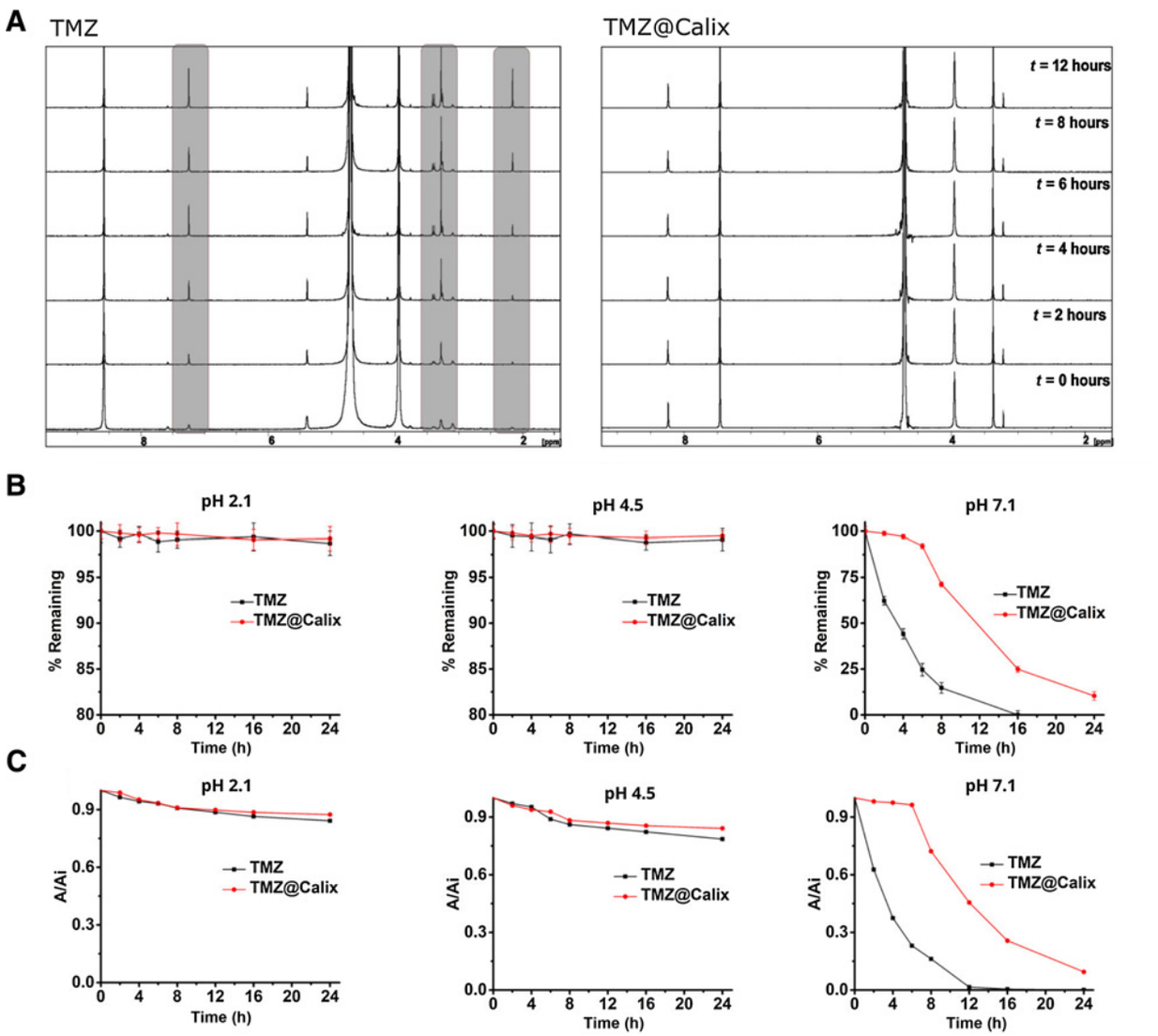

Figure 2.

Stability profiles of native TMZ and TMZ@Calix *in vitro*. **A,** ^{1}H NMR spectra of the time-dependent degradation of native TMZ and TMZ@Calix to MTIC at deuterated phosphate buffer in D_2O (10 μm). The highlighted gray peak at 7.23 ppm represents the 7-H proton of the MTIC form. The highlighted peaks at 3.52 ppm represent the 1-H proton of the MTIC form and its adduct. **B,** Stability of TMZ and TMZ@Calix under different pH conditions as monitored by LC-MS/MS. **C,** Stability of TMZ and TMZ@Calix under different pH conditions as monitored by UV–Vis.

Published OnlineFirst June 18, 2019; DOI: 10.1158/1535-7163.MCT-18-1250

to 6.4 in the duodenum, 4.4 to 6.6 in the jejunum, and 6.5 to 7.4 in the ileum (36). Both analytical techniques show that TMZ remains stable after 24-hour incubation at pH 2.1 and 4.5, whether free or encapsulated. However, at pH 7.1, native TMZ demonstrated a high rate of hydrolysis. Only around 60% of the initial concentration remained after 2 hours of incubation. Notably, encapsulation of TMZ in the TMZ@Calix complex profoundly enhanced its stability, delaying hydrolysis by more than 6 hours and increasing the half-life 4-fold under these conditions.

TMZ@Calix is significantly more effective at inhibiting the growth of GBM cells

We next proceeded to test the *in vitro* cytotoxicity of native TMZ and TMZ@Calix against GBM cells. Established (U87/8MG) and patient-derived primary GBM cultures (GBM31/GBM59/GBM77) were initially analyzed for *MGMT* expression by qPCR, an important determinant of cellular sensitivity to TMZ (Fig. 3A). We then treated these cells with varying concentrations of TMZ and analyzed them for proliferation (Fig. 3B). The *MGMT* expression was near to undetectable in the established cell lines and both were sensitive to TMZ treatment with IC_{50} doses of 5 μmol/L and 10 μmol/L for U87 and 8MG, respectively. The primary lines all expressed *MGMT* and were highly resistant to TMZ with IC_{50} values of over 300 μmol/L. Having established the sensitivity of GBM cells to native TMZ, the efficacy of the TMZ@Calix complex was tested in these cell lines using equimolar concentrations equivalent to TMZ IC_{50} doses (Fig. 3C). In 8MG and U87, TMZ@Calix reduced the number of cells by 43% ($P < 0.0001$) and 54% ($P < 0.0001$), respectively, when compared with equimolar concentrations of native TMZ. Calixarene alone had no significant effect on the growth of either cell line.

Patient-derived primary GBM cell cultures were used to validate the enhanced efficacy of TMZ@Calix. GBM31, GBM59, and GBM77 were analyzed by the CCK8 assay 9 days post-treatment TMZ@Calix at equimolar concentrations equivalent to 100 and 200 μmol/L of native TMZ. Although TMZ treatment at high concentrations did not significantly impact the TMZ-resistant primary GBM cultures, the equivalent of 100 μmol/L of TMZ encapsulated in the TMZ@Calix complex caused a highly significant 65% reduction in the proliferation of GBM31 ($P < 0.0001$), a 74% reduction of GBM59 ($P < 0.0001$) and an 81% reduction of GBM77 ($P < 0.0001$), despite these cells expressing high levels of *MGMT* (Fig. 3D).

Encapsulation greatly increases the biological half-life of TMZ and improves its therapeutic efficacy *in vivo*

The *in vivo* degradation rates of native TMZ and the TMZ@Calix complex were examined by LC-MS/MS plasma stability assays

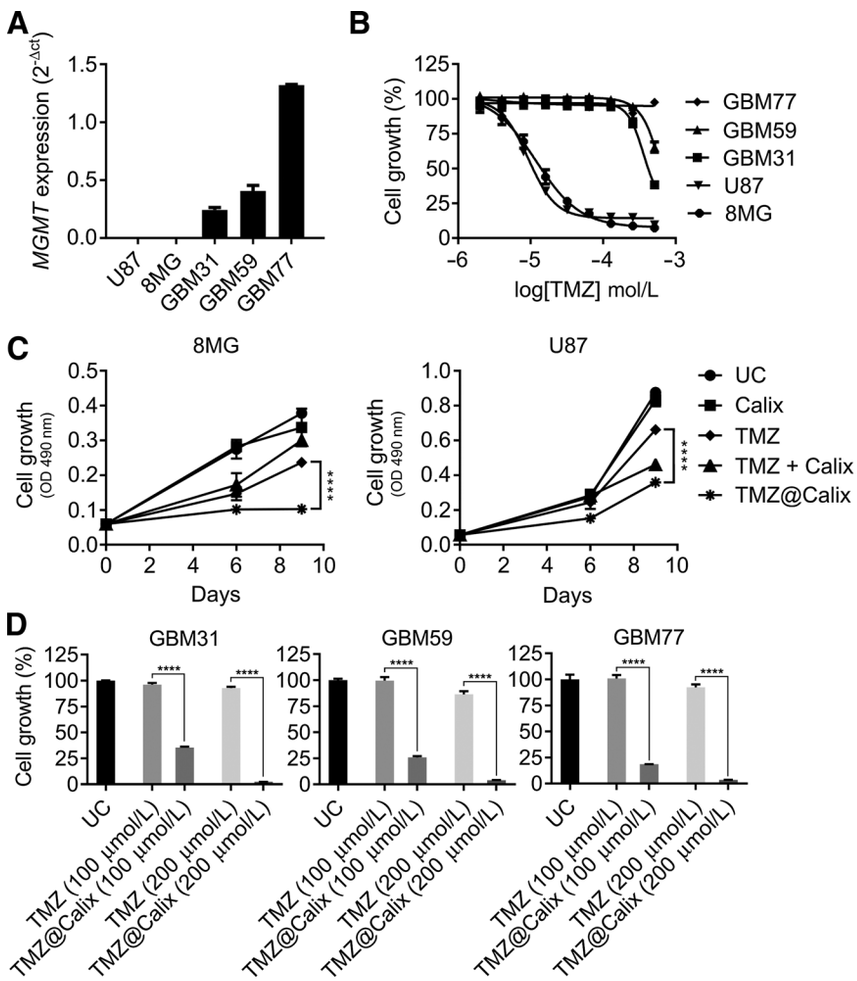

Figure 3.

MGMT expression profiling and functional assessment of TMZ and TMZ@Calix on the proliferation of GBM cell lines. **A,** *MGMT* expression determined by qPCR and represented as $2^{-\Delta ct}$. **B,** Dose response for TMZ-treated GBM cell lines (U87/8MG) and patient-derived primary cells (GBM31/GBM59/GBM77) determined by SRB assay 9 days post-treatment. TMZ concentrations used were 2, 4, 8, 16, 32, 64, 128, 256, and 512 μmol/L. Absorbance was normalized to the untreated control and represented on a log scale. **C,** Cell growth SRB assay on established GBM cell lines 8MG and U87. Cells were treated with IC_{50} doses of TMZ (U87: 5 μmol/L; 8MG: 10 μmol/L) and calixarene (U87: 13.5 μmol/L; 8MG: 27 μmol/L) both alone and in combination at equimolar concentrations to those found in the amount of TMZ@Calix complex used. The concentration of TMZ in the complex was 100 μg TMZ/mg of complex. Cells were analyzed on 6 and 9 days post-treatment. Both 8MG and U87 are *MGMT* negative and sensitive to TMZ. **D,** CCK8 assay to measure the growth of GBM primary cultures GBM31, GBM59, and GBM77, 9 days post-treatment. Cells were treated with 100 μmol/L and 200 μmol/L TMZ and the respective equimolar concentrations of the TMZ@Calix complex. Both primaries are *MGMT* positive and very resistant to TMZ. Two-way ANOVA with Tukey multiple comparisons test was used to identify significant differences between treatment groups (****, $P < 0.0001$).

Published OnlineFirst June 18, 2019; DOI: 10.1158/1535-7163.MCT-18-1250

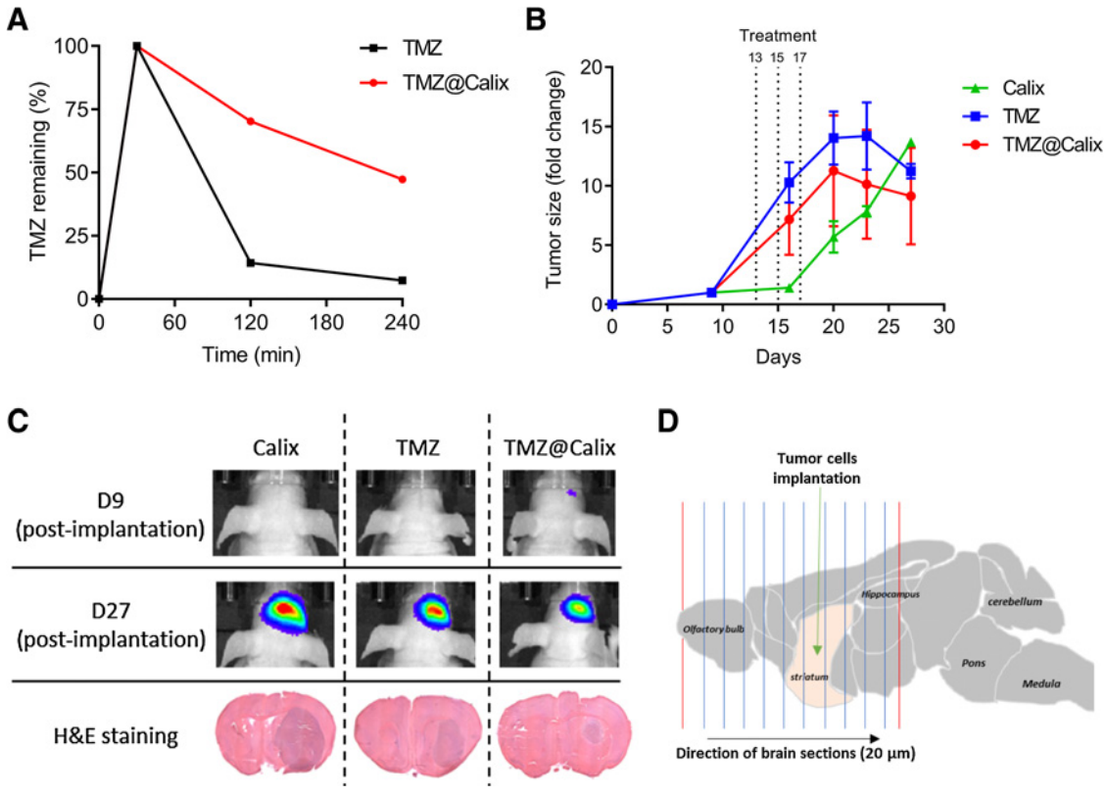

Figure 4.

Degradation profile of TMZ and TMZ@Calix and assessment of their therapeutic efficacy in an intracranial model of GBM. **A,** *In vivo* degradation rate in mouse plasma of 30 mg/kg native TMZ and equimolar TMZ encapsulated in the TMZ@Calix complex. Plasma samples were analyzed by an optimized LC-MS/MS stability assay. **B,** Therapeutic efficacy of the TMZ@Calix complex was evaluated to determine whether increased stability increases its efficacy compared with unbound TMZ. CD1 Swiss nude mice with intracranial U87 xenograft tumors were randomized into 3 groups on day 10 post-implantation ($n = 4$): p-sulphonatocalix[4]arene only control (175.5 mg/kg), TMZ (30 mg/kg), and TMZ@Calix complex (205.5 mg/kg). Prior to each treatment mice were weighed, and the dose was adjusted accordingly. Mice were imaged for luciferase activity by bioluminescence imaging on days 9, 16, 20, 24, and 27 post-implantation. Treatments were administered on days 13, 15, and 17 days post-implantation of U87 GBM cells by intraperitoneal injection. The graph shows fold change in tumor size calculated by normalizing to the bioluminescent image values of each mouse at day 9 post-implantation to account for variability in initial tumor formation. **C,** Representative images for bioluminescence at days 9 and 27 post-implantation and representative H&E images from animals in each treatment group. **D,** Schematic representation of how brains were sectioned. The H&E stains in **D** represent sections taken from the largest area of the tumor bulk.

(Fig. 4A). Mice were intraperitoneally injected with 30 mg/kg TMZ and an equimolar dose of the TMZ@Calix complex (205.5 mg/kg) and blood collected by cardiac puncture pretreatment (0) and at 30 minutes, 2 hours, and 4 hours post-treatment. As previously reported, we found the half-life of native TMZ to be very short with only 8% of the injected dose remaining 4 hours post-administration. In contrast, 47% of the TMZ administered as the TMZ@Calix complex could be detected at this time point.

To determine if this enhanced stability would lead to greater efficacy, the complex was tested for its therapeutic potential in an intracranial GBM mouse model using U87 GBM cells (Fig. 4B). Groups of 4 mice were treated with calixarene only as a control (175.5 mg/kg), native TMZ (30 mg/kg), or the TMZ@Calix complex (205.5 mg/kg). Mice were treated on days 13, 15, and 17 post-implantation and then sacrificed on day 28. Bioluminescence imaging revealed enhanced tumor shrinkage in mice treated with the TMZ@Calix complex compared with those treated with native TMZ or calixarene alone; however, these results appeared not to be significant (Fig. 4C). Upon further inspection of the brains by H&E staining of the largest area of the tumor (Fig. 4D), there was clear indication of an enhanced therapeutic effect in mice treated with the TMZ@Calix complex where the tumor size was drastically reduced compared with native TMZ (Fig. 4C, bottom).

Discussion

Parenchymal brain tumors present unique management challenges because of their inherent aggressiveness, cellular heterogeneity, and location. Although developments in detection methods, surgical techniques, and radiology have contributed to a modestly improved clinical outcome, there has been little progress in the development of chemotherapeutics. Since its introduction to the clinic in 2007, TMZ has remained the standard-of-care systemic therapy for brain tumors, especially for GBM. Notwithstanding promising developments, for example in immunotherapy, TMZ will remain an essential agent in the management of GBM for the foreseeable future (37). With TMZ now being off patent, it is the ideal time to modify this drug to develop a more efficacious and cost-effective treatment.

Published OnlineFirst June 18, 2019; DOI: 10.1158/1535-7163.MCT-18-1250

Here, TMZ was encapsulated to form a TMZ@Calix complex in which TMZ is protected from rapid degradation. Native TMZ has a half-life of 1.83 hours at 37°C in phosphate buffer (0.1 M) at pH 7 (38). Evaluation of TMZ@Calix dissociation and stability according to FDA and EMA guidelines confirmed that the hydrolysis of TMZ to its active compound, MITC, is significantly delayed (32). This stabilization far exceeds what has been achieved by a previous study, where UV–Vis spectrometry in a 10 mmol/L buffer solution at pH 7.0 showed an extension of the TMZ half-life by around 2 hours when complexed to cucurbit[7]uril (39). By forming a complex with Calix, we extended the half-life to more than 12 hours. The stability of TMZ is therefore enhanced 4-fold by encapsulating it in a TMZ@Calix complex. Because the therapeutic action of TMZ requires induction of sufficient DNA damage to result in cell death, we determined whether the enhanced stability results in increased chemotherapeutic efficacy and we show that *in vitro* the TMZ@Calix complex is a significantly more potent inhibitor of tumor cell growth than native TMZ.

Particularly striking is the ability of the TMZ@Calix complex to inhibit tumor cell growth even in those primary GBM cells that express high levels of *MGMT* and are normally refractory to therapy. Importantly, we have demonstrated activity of TMZ@Calix in three independent MGMT-positive early passage primary GBM cultures. This clearly strengthens the general applicability of our findings, which is in line with a previous publication where platinum-based drugs were stabilized by complexing with para-sulfonato-calix[4]arene, resulting in increased anticancer activity in a cisplatin-resistant ovarian cancer cell line (30). Overcoming MGMT-mediated innate TMZ resistance would be of major significance in GBM treatment considering that approximately 60% of patients express *MGMT* and therefore do not benefit from TMZ treatment (6). It was observed that the TMZ@Calix complex affects cells earlier than unbound TMZ, which suggests increased cellular uptake. The combination of enhanced cell uptake with increased stability could explain how the TMZ@Calix complex is able to overcome MGMT-mediated TMZ resistance. Surprisingly, little is known about the cellular uptake of TMZ and the kinetics involved, but Calix has been characterized in terms of its cellular uptake and has been found to enter cells very efficiently and to accumulate in the cytoplasm (40). In that study, a fluorescently labeled calix[4]arene was used where the fluorescent intensity changes from weak to strong upon conjugation (40). This method could also be used in future studies to assess the cellular uptake of the TMZ@Calix complex to better understand the kinetics behind its enhanced antitumor effects.

Having demonstrated that encapsulation potentiates the *in vitro* stability and antitumor activity of TMZ, we next tested the *in vivo* pharmacokinetic and therapeutic properties in mice. We demonstrated that encapsulation of TMZ with calixarene greatly enhanced its stability in plasma and improved its therapeutic efficacy in an orthotopic model of GBM far superior to native TMZ. The increased ability of the TMZ@Calix complex to inhibit intracranial GBM is particularly striking because a previous study reported that unbound para-sulfonato-calix[4]arene do not enter the brain of mice even at high concentrations of 100 mg/kg (23). A possible explanation for the higher potency observed with TMZ@Calix is that through enhanced stability provided by para-sulfonato-calix[4]arene, higher concentrations of released TMZ will pass through the BBB and enter the tumor site. Moreover, encapsulated TMZ may indeed be able to enter the perturbed BBB increasing the local concentration of TMZ in the brain. Further *in vivo* biodistribution studies will be performed to evaluate the accumulation of TMZ in the brain when administered complexed to calixarene. Orthotopic models of *MGMT* expressing primary human GBM cells will also be used to further understand the enhanced therapeutic efficacy of TMZ@Calix.

There are several other approaches that could be taken to further enhance the antitumor efficacy of the TMZ@Calix complex. For example, coassembly of amphiphilic p-sulphonatocalix[4]arenes into multifunctional drug carriers that can be functionalized by decorating them with tumor targeting ligands have been explored in recent years, and this approach could also be used to deliver TMZ (41, 42). The TMZ@Calix complex could also be functionalized with a potent MGMT inhibitor to further enhance its efficacy against *MGMT*-expressing TMZ-resistant tumors (43). TMZ has also been conjugated directly to compounds where coadministration causes a synergistic antitumor effect. For example, a conjugate of TMZ and perillyl alcohol termed NEO212 was found to be 10-fold more cytotoxic than TMZ alone (44). Instead of using conventional TMZ, NEO212 could be loaded onto calixarene to enhance its stability, efficacy, and ease of delivery. Finally, the TMZ@Calix complex could additionally be functionalized by conjugation to angiopep-2, to further enhance active transport across the BBB, as has been reported for angiopep-2 functionalized nanoparticles targeting glioma (45–47). This small peptide has been shown to cross the BBB in animal models via transcytosis by binding to low density lipoprotein receptor-related protein (LRP) expressed on the surface of the BBB. Moreover, GBM cell lines have been reported to express LRP (48).

These options are currently being explored in our labs because we believe this method of TMZ stabilization to be a significant enhancement to the current standard of care with potentially broad treatment implications.

To date, there has been only one clinical trial listed involving p-sulphonatocalix[4]arenes: OTX-008 is a synthetic p-sulphonatocalix[4]arene molecule that binds directly to galectin-1 and induces a conformational change reducing the binding to carbohydrates. Promising pharmacokinetic data were presented in an abstract at the AACR 104th annual meeting in 2013 (49). With preliminary clinical trial data on the synthetic p-sulphonatocalix[4]arene OTX-008 having been positive and the preclinical indications that Calix can function as nontoxic drug carrier (49), we anticipate that the TMZ@Calix complex could quickly move through clinical trials with more robust *in vivo* testing. Due to the lengthy processes involved in translating completely novel effective therapies for GBM treatment, we envisage that the TMZ@Calix complex could be an inexpensive and highly potent treatment option made readily available to GBM patients in the near future.

Disclosure of Potential Conflicts of Interest

No potential conflicts of interest were disclosed.

Authors' Contributions

Conception and design: A. Renziehausen, A.D. Tsiailanis, T. Crook, A.G. Tzakos, N. Syed

Development of methodology: A. Renziehausen, A.D. Tsiailanis, E.K. Stylos, C. Chatzigiannis, A.G. Tzakos, N. Syed

Published OnlineFirst June 18, 2019; DOI: 10.1158/1535-7163.MCT-18-1250

Analysis and interpretation of data (e.g., statistical analysis, biostatistics, computational analysis): A. Renziehausen, A.D. Tsiailanis, R. Perryman, C. Chatzigiannis, T. Crook, A.G. Tzakos, N. Syed
Writing, review, and/or revision of the manuscript: A. Renziehausen, A.D. Tsiailanis, R. Perryman, E.K. Stylos, T. Crook, A.G. Tzakos, N. Syed
Administrative, technical, or material support (i.e., reporting or organizing data, constructing databases): R. Perryman, N. Syed
Study supervision: K. O'Neill, A.G. Tzakos, N. Syed

Acknowledgments

This work was funded by the Barrow Neurological Foundation UK (awarded to N. Syed to support the PhD studentship for A. Renziehausen), the Brain Tumour Research Campaign (project grant awarded to N.Syed), and the Brain Tumour Research (project grant awarded to K. O'Neill and N. Syed).

The costs of publication of this article were defrayed in part by the payment of page charges. This article must therefore be hereby marked *advertisement* in accordance with 18 U.S.C. Section 1734 solely to indicate this fact.

Received November 3, 2018; revised April 12, 2019; accepted June 11, 2019; published first June 18, 2019.

References

1. Stupp R, Mason WP, van den Bent MJ, Weller M, Fisher B, Taphoorn MJ, et al. Radiotherapy plus concomitant and adjuvant temozolomide for glioblastoma. N Engl J Med 2005;352:987–96.
2. Stupp R, Hegi ME, Mason WP, wan den Bent MJ, Taphoorn MJ, Janzer RC, et al. Effects of radiotherapy with concomitant and adjuvant temozolomide versus radiotherapy alone on survival in glioblastoma in a randomised phase III study: 5-year analysis of the EORTC-NCIC trial. Lancet Oncol 2009;10:459–66.
3. Roos WP, Batista LF, Naumann SC, Wick W, Weller M, Menck CF, et al. Apoptosis in malignant glioma cells triggered by the temozolomide-induced DNA lesion O6-methylguanine. Oncogene 2007;26:186–97.
4. Weller M, Tabatabai G, Kastner B, Felberg J, Steinbach JP, Wick A, et al. MGMT promoter methylation is a strong prognostic biomarker for benefit from dose-intensified temozolomide rechallenge in progressive glioblastoma: the DIRECTOR trial. Clin Cancer Res 2015;21:2057–64.
5. Happold C, Roth P, Wick W, Schmidt N, Florea AM, Silginer M, et al. Distinct molecular mechanisms of acquired resistance to temozolomide in glioblastoma cells. J Neurochem 2012;122:444–55.
6. Hegi ME, Diserens AC, Gorlia T, Hamou MF, de Tribolet N, Weller M, et al. MGMT gene silencing and benefit from temozolomide in glioblastoma. N Engl J Med 2005;352:997–1003.
7. Zhou Q, Guo P, Wang X, Nuthalapati S, Gallo JM. Preclinical pharmacokinetic and pharmacodynamic evaluation of metronomic and conventional temozolomide dosing regimens. J Pharmacol Exp Ther 2007;321:265–75.
8. Portnow J, Badie B, Chen M, Liu A, Blanchard S, Synold TW. The neuropharmacokinetics of temozolomide in patients with resectable brain tumors: potential implications for the current approach to chemoradiation. Clin Cancer Res 2009;15:7092–8.
9. Lopes IC, De Oliveira SCB, Oliveira-Brett AM. Temozolomide chemical degradation to 5-aminoimidazole-4-carboxamide – electrochemical study. J Electroanal Chem 2013;704:183–9.
10. Meer L, Janzer RC, Kleihues P, Kolar GF. In vivo metabolism and reaction with dna of the cytostatic agent, 5-(3,3-dimethyl-1-triazeno)imidazole-4-carboxamide (DTIC). Biochem Pharmacol 1986;35:3243–7.
11. Ostermann S, Csajka C, Buclin T, Leyvraz S, Lejeune F, Decosterd LA, et al. Plasma and cerebrospinal fluid population pharmacokinetics of temozolomide in malignant glioma patients. Clin Cancer Res 2004;10:3728–36.
12. Fang C, Wang K, Stephen ZR, Mu Q, Kievit FM, Chiu DT, et al. Temozolomide nanoparticles for targeted glioblastoma therapy. ACS Appl Mater Interfaces 2015;7:6674–82.
13. Tian XH, Lin XN, Wei F, Feng W, Huang ZC, Wang P, et al. Enhanced brain targeting of temozolomide in polysorbate-80 coated polybutylcyanoacrylate nanoparticles. Int J Nanomed 2011;6:445–52.
14. Hu J, Wang J, Wang G, Yao Z, Dang X. Pharmacokinetics and antitumor efficacy of DSPE-PEG2000 polymeric liposomes loaded with quercetin and temozolomide: analysis of their effectiveness in enhancing the chemosensitization of drug-resistant glioma cells. Int J Mol Med 2016;37:690–702.
15. Irani M, Mir Mohamad Sadeghi G, Haririan I. Gold coated poly (ε-caprolactonediol) based polyurethane nanofibers for controlled release of temozolomide. Biomed Pharmacother 2017;88:667–76.
16. Irani M, Mir Mohamad Sadeghi G, Haririan I. A novel biocompatible drug delivery system of chitosan/temozolomide nanoparticles loaded PCL-PU nanofibers for sustained delivery of temozolomide. Int J Biol Macromol 2017;97:744–51.
17. Di Martino A, Kucharczyk P, Capakova Z, Humpolicek P, Sedlarik V. Enhancement of temozolomide stability by loading in chitosan-carboxylated polylactide-based nanoparticles. J Nanoparticle Res 2017;19:17
18. Clemente N, Ferrara B, Gigliotti CL, Boggio E, Capucchio MT, Biasibetti, et al. Solid lipid nanoparticles carrying temozolomide for melanoma treatment. preliminary in vitro and in vivo studies. Int J Mol Sci 2018;9:255.
19. Patil R, Portilla-Arias J, Ding H, Inoue S, Konda B, Hu J, et al. Temozolomide delivery to tumor cells by a multifunctional nano vehicle based on poly(β-L-malic acid). Pharm Res 2010;27:2317–29.
20. Kumari S, Ahsan SM, Kumar JM, Kondapi AK, Rao NM. Overcoming blood brain barrier with a dual purpose temozolomide loaded lactoferrin nanoparticles for combating glioma (SERP-17-12433). Sci Rep 2017;7:6602.
21. Blanco E, Shen H, Ferrari M. Principles of nanoparticle design for overcoming biological barriers to drug delivery. Nat Biotechnol 2015;33:941–51.
22. Perret F, Coleman AW. Biochemistry of anionic calix[n]arenes. Chem Commun 2011;47:7303–19.
23. Coleman AW, Jebors S, Cecillon S, Perret P, Garin D, Marti-Battle D, et al. Toxicity and biodistribution of para-sulfonato-calix[4]arene in mice. New J Chem 2008;32:780.
24. Da Silva E, Shahgaldian P, Coleman AW. Haemolytic properties of some water-soluble para-sulphonato-calix-[n]-arenes. Int J Pharm 2004;273:57–62.
25. Paclet MH, Rousseau CF, Yannick C, Morel F, Coleman AW. An absence of non-specific immune response towards para-sulphonato-calix[n]arenes. J Incl Phenom Macrocycl Chem 2006;55:353–7.
26. Guo DS, Wang K, Liu Y. Selective binding behaviors of p-sulfonatocalixarenes in aqueous solution. J Incl Phenom Macrocycl Chem 2008;62:1–21.
27. Karakurt S, Kellici TF, Mavromoustakos T, Tzakos AG, Yilmaz M. Calixarenes in lipase biocatalysis and cancer therapy. Curr Org Chem 2016;20:1043–57.
28. Mo J, Eggers PK, Yuan ZX, Raston CL, Lim LY. Paclitaxel-loaded phosphonated calixarene nanovesicles as a modular drug delivery platform. Sci Rep 2016;6:23489
29. Galindo-Murillo R, Olmedo-Romero A, Cruz-Flores E, Petrar PM, Kunsagi-Mate S, Barroso-Flores J. Calix[n]arene-based drug carriers: a DFT study of their electronic interactions with a chemotherapeutic agent used against leukemia. Comput Theor Chem 2014;1035:84–91.
30. Brown SD, Plumb JA, Johnston BF, Wheate NJ. Folding of dinuclear platinum anticancer complexes within the cavity of para-sulphonatocalix[4]arene. Inorganica Chim Acta 2012;393:182–6.
31. Yousaf A, Hamid SA, Bunnori NM, Ishola AA. Applications of calixarenes in cancer chemotherapy: facts and perspectives. Drug Des Devel Ther 2015;9:2831–8.
32. Ishaq BM, Ahad HA, Muneer S, Parveen S, Fahmida B. Analytical method development and validation for the estimation of temozolomide in phosphate buffer ph 2.0 as a solvent by UV spectroscopy. Int Res J Pharm 2014;5:7–20.

Published OnlineFirst June 18, 2019; DOI: 10.1158/1535-7163.MCT-18-1250

33. Verbeeck RK, Musuamba FT. The revised 2010 EMA guideline for the investigation of bioequivalence for immediate release oral formulations with systemic action. J Pharm Pharm Sci 2012;15:376–88.
34. Syed N, Langer J, Janczar K, Janczar K, Singh P, Lo Nigro C, et al. Epigenetic status of argininosuccinate synthetase and argininosuccinate lyase modulates autophagy and cell death in glioblastoma. Cell Death Dis 2013;4: e458.
35. El Mubarak MA, Stylos EK, Chatziathanasiadou MV, Danika C, Alexiou GA, Tsekeris P, et al. Development and validation of simple step protein precipitation UHPLC-MS/MS methods for quantitation of temozolomide in cancer patient plasma samples. J Pharm Biomed Anal 2019; 162:164–70.
36. Riethorst D, Mols R, Duchateau G, Tack J, Brouwers J, Augustijns P. Characterization of human duodenal fluids in fasted and fed state conditions. J Pharm Sci 2016;105:673–81.
37. Chamberlain MC, Kim BT. Nivolumab for patients with recurrent glioblastoma progressing on bevacizumab: a retrospective case series. J Neurooncol 2017;133:561–9.
38. Wheelhouse RT, Stevens MFG. Decomposition of the antitumour drug temozolomide in deuteriated phosphate buffer: Methyl group transfer is accompanied by deuterium exchange. J Chem Soc Chem Commun 1993; 15:1177–8.
39. Appel EA, Rowland MJ, Loh XJ, Heywood RM, Watts C, Scherman OA. Enhanced stability and activity of temozolomide in primary glioblastoma multiforme cells with cucurbit[n]uril. Chem Commun 2012;48: 9843.
40. Lalor R, Baillie-Johnson H, Redshaw C, Matthews SE, Mueller A. Cellular uptake of a fluorescent calix[4]arene derivative. J Am Chem Soc 2008;130: 2892–3.
41. Eggers PK, Becker T, Melvin MK, Boulos RA, James E, Morellini N, et al. Composite fluorescent vesicles based on ionic and cationic amphiphilic calix[4]arenes. RSC Adv 2012;2:6250.
42. Wang YX, Guo DS, Duan YC, Wang YJ, Liu Y. Amphiphilic p-sulfonatocalix[4]arene as "drug chaperone" for escorting anticancer drugs. Sci Rep 2015;5:9019.
43. Wang C, Abegg D, Hoch DG, Adibekian A. Chemoproteomics-enabled discovery of a potent and selective inhibitor of the DNA repair protein MGMT. Angew Chem Int Ed Engl 2016;55:2911–5.
44. Jhaveri N, Agasse F, Armstrong D, Peng L, Commins D, Wang W, et al. A novel drug conjugate, NEO212, targeting proneural and mesenchymal subtypes of patient-derived glioma cancer stem cells. Cancer Lett 2016; 371:240–50.
45. Gao H, Zhang S, Cao S, Yang Z, Pang Z, Jiang X. Angiopep-2 and activatable cell-penetrating peptide dual-functionalized nanoparticles for systemic glioma-targeting delivery. Mol Pharm 2014;11:2755–63.
46. Wang L, Hao Y, Li H, Zhao Y, Meng D, Li D, et al. Co-delivery of doxorubicin and siRNA for glioma therapy by a brain targeting system: angiopep-2-modified poly(lactic-co-glycolic acid) nanoparticles. J Drug Target 2015;23:832–46.
47. Figueiredo P, Balasubramanian V, Shahbazi MA, Correia A, Wu D, Palivan DG, et al. Angiopep2-functionalized polymersomes for targeted doxorubicin delivery to glioblastoma cells. Int J Pharm 2016;511:794–803.
48. Malentinska L, Blakely EA, Bjornstad KA, Deen DF, et al. Human glioblastoma cell lines: levels of low density lipoprotein receptor and low density lipoprotein receptor-related protein. Cancer Research 2000;60:2300–3.
49. Rezai K, Durand S, Lachaux N, Raymond E, Herait P, Lokiec F. Abstract 33: OTX008 pharmacokinetics (PK) during the first-in-man phase I study in patients with advanced solid tumors. Cancer Res 2013;73:33.

AACR American Association for Cancer Research

Molecular Cancer Therapeutics

Encapsulation of Temozolomide in a Calixarene Nanocapsule Improves Its Stability and Enhances Its Therapeutic Efficacy against Glioblastoma

Alexander Renziehausen, Antonis D. Tsiailanis, Richard Perryman, et al.

Mol Cancer Ther 2019;18:1497-1505. Published OnlineFirst June 18, 2019.